Polymer 49 (2008) 4666–4672

Contents lists available at ScienceDirect

Polymer

journal homepage: www.elsevier.com/locate/polymer

Study of the thermal conduction mechanism of nano-SiC/DGEBA/EMI-2,4 composites

Tianle Zhou [a,b,*], Xin Wang [a], G.U. Mingyuan [c], Xiaoheng Liu [a]

[a] Key Laboratory for Soft Chemistry and Functional Materials of Ministry Education, Nanjing University of Science and Technology, Nanjing 210094, China
[b] Department of Materials Science and Engineering, Nanjing University of Science and Technology, Nanjing 210094, China
[c] State Key Laboratory of MMCs, Shanghai Jiao Tong University, Shanghai 200240, China

ARTICLE INFO

Article history:
Received 27 March 2008
Received in revised form 30 July 2008
Accepted 13 August 2008
Available online 16 August 2008

Keywords:
Thermal conduction mechanism
Nano-SiC/DGEBA/EMI-2,4 composites
FTIR

ABSTRACT

This report covers the results of a study on identifying the thermal conduction mechanism of nano-sized SiC/diglycidyl ether of bisphenol-A glycidol ether epoxy resin/2-ethyl-4-methylimidazole (nano-SiC/DGEBA/EMI-2,4) composites. The analysis using FTIR provided an in-depth understanding about how the pretreatment of micro/nano-sized SiC (micro/nano-SiC) particles affects the surface structure of the two different-sized particles, and thereby results in the difference in particles/resin interface structures, which determine different thermal conduction mechanisms. The surface modification approaches included: (1) silane treatment using γ-aminopropyl-triethoxysilane (A1100) and (2) oxidation followed by silane treatment. The results showed that, it is the structure of cross-linked SiC particles/resin three-dimensional network, established by chemical bonding, dominates the thermal conduction mechanism of nano-SiC/DGEBA/EMI-2,4 composites, and leads to the nanocomposites with high thermal conductivity at low filler content. Meanwhile, thermal conduction chains, the prevailing thermal conduction mean in the micro-SiC/DGEBA/EMI-2,4 composites, are the secondary means to conduct thermal diffusion in the nanocomposites.

1. Introduction

With the strong progress in nanomaterials and nanotechnology, studies on the properties of nano-inorganic/polymer nanocomposites have been developed rapidly. It is well known that the interface structure of composites plays an important role in properties especially when the interface thickness can be compared to the size of the filler. Therefore, studies on properties stimulate an increasing interest in investigating the interface structure between nanofillers and polymer matrix, which helps to identify the mechanisms involved in the improvement of properties, such as thermal conductivity. In the case of microfiller/polymer composites, the thermal conduction mechanism, explained by the established percolation theory [1–3], has already been widely accepted, namely, thermal conduction chains conduct thermal diffusion. There is an onset of thermal conductivity when filler content exceeds the critical value, commonly named percolation threshold, to form at least one continuous thermal conduction chain, viz., effective thermal conductive pathway, connecting the opposite faces of matrix. Although the research work involving the thermal conductivity of nanocomposites is still widely unexplored, there has been some research work involved in the thermal conduction mechanism of nanocomposites, such as that of the carbon nanotube/epoxy composites [4], however, the thermal conduction mechanism of nano-SiC/DGEBA/EMI-2,4 composites has not been studied in detail.

SiC is very attractive due to the fact that it has a number of interesting properties such as high thermal conductivity, low coefficient of thermal expansion, etc. These characteristics make it possible to design and fabricate high performance particle-laden polymer composites. In this paper, SiC particles with average particle size of 50 nm and 0.75 μm were used with DGEBA/EMI-2,4 system as the base system.

Owing to the ultrafine dimension of nanoparticles, a large fraction of atoms can reside at the interface, leading to a strong interfacial interaction if a homogeneous dispersion of nanofillers in polymer matrix is guaranteed, thus the nanocomposites coupled with a great number of interfaces can be expected to provide unusual performance. In fact, physical mixtures of inorganic nanoparticles and polymers would weaken the properties of the resultant materials due to nanoparticle agglomeration and poor particles/matrix interfacial interaction. Nanoparticle agglomerates with a great number of interfaces, which bring high interfacial thermal resistance, are detrimental to thermal conductivity of

* Corresponding author. Key Laboratory for Soft Chemistry and Functional Materials of Ministry Education, Nanjing University of Science and Technology, Nanjing 210094, China. Tel.: +86 02 58 431 5325; fax: +86 02 58 431 3421.
E-mail address: ztltianle999@hotmail.com (T. Zhou).

0032-3861/$ – see front matter © 2008 Elsevier Ltd. All rights reserved.
doi:10.1016/j.polymer.2008.08.023

polymer composites. Whereas surface modification of the nanoparticles has already been proved to be a wide applicable technique to prevent from the aggregation of nanoparticles and enhance particle/matrix interfacial interaction [5]. Enhanced particle/matrix interfacial adhesion via chemical bonding is effective way to decrease interfacial thermal resistance [6,7]. As far as silane treatment is concerned, silane coupling agent contains both organic and inorganic functionalities, allowing it to act as a chemical bridge between two dissimilar materials, so it is often used to enhance interfacial adhesion between hydrophilic inorganic oxides and hydrophobic polymer resins, as well as preventing from the agglomeration of nanoparticles [8]. Furthermore, Neyman et al. reported that XPS results suggested that further enhanced adhesive bonding of an epoxy to SiC is due to the formation of a thicker oxide layer caused by oxygen plasma pretreatment prior to the silane treatment [9]. In this study, surface modifications of SiC particles included silane treatment using A1100 and oxidation treatment followed by silane treatment.

The purpose of this paper is to provide an in-depth understanding about how the pretreatment of micro/nano-SiC particles affects the surface structure of the two different-sized particles, and thereby results in the difference in particles/resin interface structures, which determine different thermal conduction mechanisms. This study contributes to the better understanding of the process–structure–properties relationship to manufacture high performance materials, and is a part of a wider investigation on high performance nanocomposites for more demanding applications, such as in microelectronics applications, etc.

2. Experimental

2.1. Materials

Epoxy resin used in this work was a nominally difunctional epoxy resin, Epon 828, supplied by Shanghai Resin Co. Epon 828 is, basically, DGEBA with epoxy value of 0.48–0.52 mol/100 g. Curing agent utilized was EMI-2,4 supplied by Beijing Chemical Reagent Co. The DGEBA/EMI-2,4 ratio employed was 100:4. β-SiC particles with average particle size of 50 nm and 0.75 μm were obtained from Karl Co. Before stored in desiccators, the particles were dried at 383 K for 24 h in vacuum to eliminate the agglomeration caused by hygroscopic absorption, as well as removing planar water, which would hinder the interaction between coupling agent and particles. Micrographs of the SiC particles are shown in Fig. 1. The nano-SiC and micro-SiC particles are seen to be approximately spherical and irregular polyhedral in shape, respectively. SiC particles without silane treatment are seriously and unevenly agglomerated. Amino silane coupling agent, γ-aminopropyl-triethoxysilane (A1100), was obtained from Shanghai Chemical Reagent Co. Other agents utilized were analytically pure grade and were supplied by Beijing Chemical Reagent Co.

2.2. Surface modification of SiC particles

Surface of SiC exhibits oxidation resistance by the formation of a passivating thin, dense and self-healing protective amorphous silica (SiO_2) film, which has extremely low oxygen permeability up to very high temperatures. Therefore, before oxidation, SiC particles were dipped in a 10 vol.% hydrofluoric acid (HF) solution for several minutes, followed by a rinse in acetone, to remove the very thin native oxide film intrinsically present on the surface of SiC particles. The oxidation of SiC results in the formation of quartz (≥973 K), tridymite (1073–1573 K), or cristobalite (≥1673 K), which are the stable crystalline polymorphs of silica (SiO_2) at ambient pressure, and the only variable affecting the occurrence of a specific polymorph is the oxidation temperature [10]. Since there are no important differences in chemical bonds of different polymorph forms of SiO_2, and the use of low temperatures is not very practical because the oxidation times become excessively long, therefore, in the present study, surface oxidation treatment of SiC particles was conducted at a moderate temperature, 1173 K, which represents a compromise between a reasonable rate and a low processing temperature, in static air at ambient pressure. In addition, the longer the oxidation time or the higher the oxidation temperature, the thicker is the oxide scale. The dependence of the oxide thickness on oxidation time is parabolic [11]. Owing to the ultrafine dimension of nano-SiC particles, the oxidation time was controlled to be relatively short, 1 h, to avoid resulting overgrown thick oxides, which would dramatically decrease the whole thermal conductivity of nano-SiC particles. Oxidation time for micro-SiC particles was set to be 20 h due to the larger dimension. Under the oxidation regimes, oxide thickness on the nano-SiC and micro-SiC particles would be thinner than 10 nm and 140 nm, respectively [11]. SiC particles were placed in the preheated furnace, and after oxidation, the oxidation products were left in the furnace, cooled to room temperature, and then were stored in desiccators.

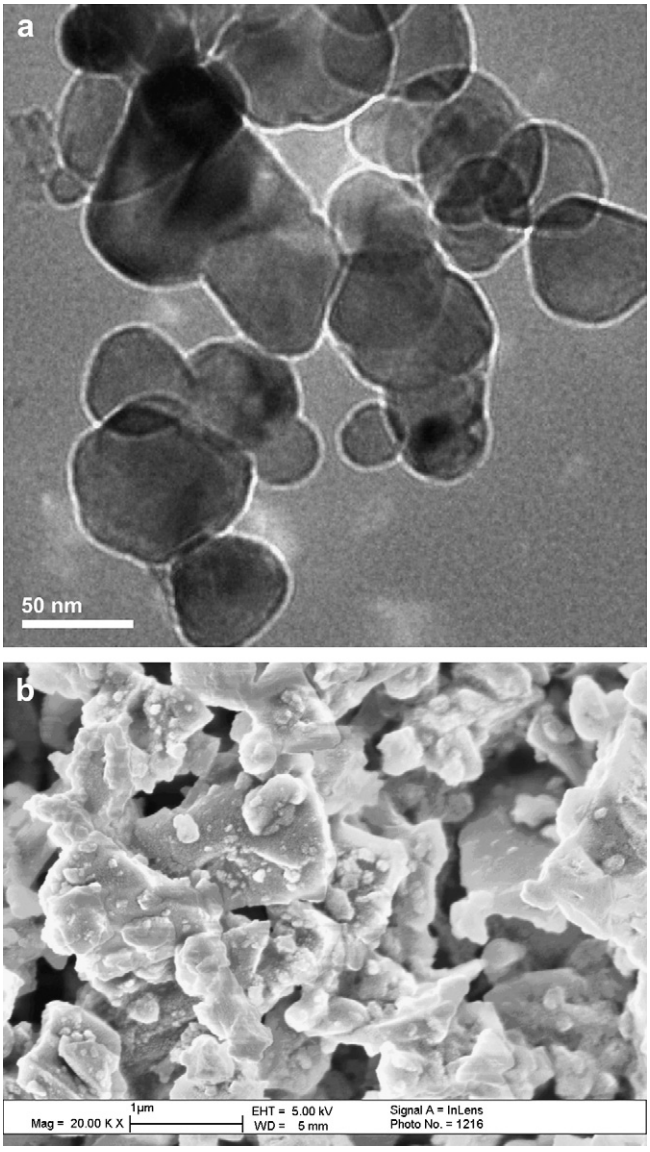

Fig. 1. (a) TEM micrograph of silane treated nano-SiC and (b) FE-SEM micrograph of as-received micro-SiC particles.

Surface treatment of SiC particles using A1100 involved (i) making a silane–absolute ethanol solution at a selected concentration, and the amounts of silane coupling agent used were 10% by weight of the nano-SiC particles and 3% by weight of the micro-SiC particles, (ii) adding oxidized or untreated SiC particles to the solution and stirring with a magnetic stirrer at 333 K for 30 min, in addition, dispersing the solution added with nanoparticles by sonication for 1 h since nanoparticles are known to agglomerate easily, (iii) rinsing with absolute ethanol by filtration, and (iv) drying at 383 K for 1 h in vacuum. Then the silane treated particles were stored in desiccators.

2.3. Composites preparation

The SiC/DGEBA/EMI-2,4 composites were prepared by solution blending and casting method, which involved (i) stirring DGEBA–absolute ethanol solution at 353 K with magnetic stirrer for 20 min, (ii) adding appropriate amount of surface treated or untreated SiC particles to the solution and continuing stir for 30 min, in addition, sonicating the solution added with nanoparticles for 1 h to ensure good homogeneity, (iii) cooling to 333 K, (iv) adding EMI-2,4, which is 4% by weight of DGEBA, to the mixture and continuing stir for 10 min, (v) casting the mixture in mould, (vi) repeatedly degassing the mixture in vacuum drying oven at 333 K until no air bubble appears on the surface of the mixture, (vii) curing the mixture at 338 K for 1 h, 393 K for 1.5 h, and 433 K for 1.5 h, and the curing time for nanocomposites should be prolonged moderately since nano-SiC particles would delay the curing reaction as reported in our previous work [12], and (viii) cooling to room temperature, then demoulding.

Micrographs of fracture surface prepared from epoxy composites with 8.6 vol.% and 14 vol.% silane treated nano-SiC particles are shown in Fig. 2a and b, respectively. The nanocomposites fail in brittle manner and silane treated nano-SiC particles are seen to be separated and uniformly embedded in the matrix. No obvious naked particles and inorganic clusters present, indicating good interfacial adhesion between the particles and polymer matrix after silane pretreatment.

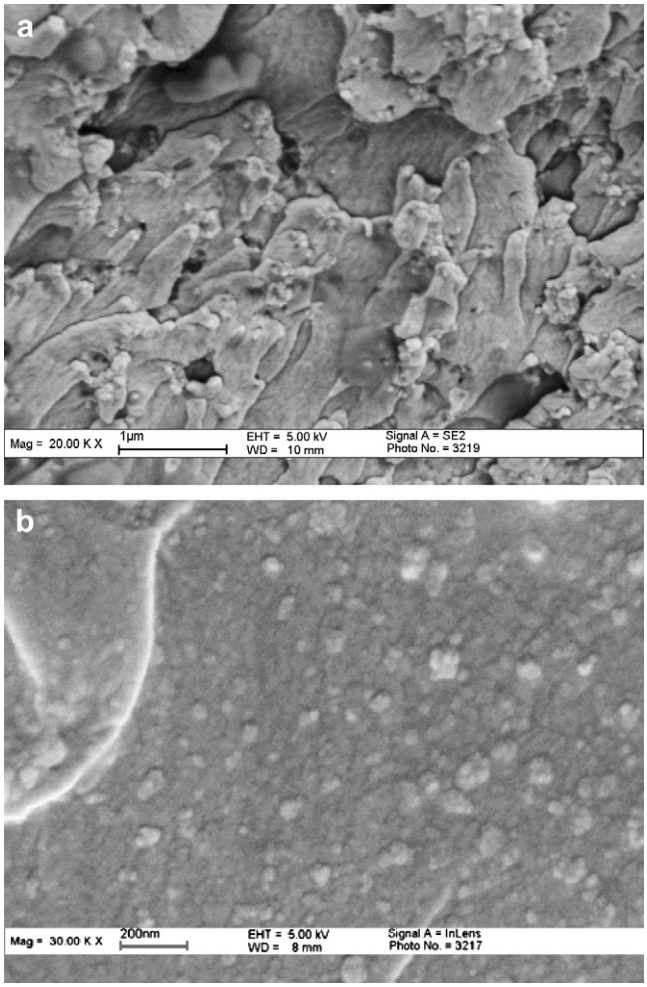

Fig. 2. FE-SEM micrographs of fracture surface of epoxy composites containing (a) 8.6 vol.% and (b) 14 vol.% silane treated nano-SiC particles.

2.4. Characterization

Fourier-transform infrared (FTIR) spectroscopy was employed to investigate the variation in the surface structure of particles and the interface structure of composites. The spectra were recorded in KBr pellets on an EQUINOX 55 spectrometer (Bruker Co., Germany). Blank scanning was performed before measurements to eliminate the influence of water vapor and CO_2 in air.

Thermal conductivity (λ, W/m K) of the composites at room temperature was given by the product of thermal diffusivity (δ, mm^2/s), specific heat (C, J/g K) and bulk density (ρ, g/cm^3).

Laser flash method for thermal diffusivity measurement is one of the most commonly used techniques for various kinds of solid, liquid and powder samples. Front surface of the sample receives a pulse of energy from the laser, which soon raises the back-face temperature. The back-face temperature response is normalized and compared with corresponding theoretical models to obtain thermal diffusivity values. This non-destructive measurement technique enjoys the advantages of using small samples of simple shapes, the ability to measure over wide temperature ranges rapidly (and hence being cost-effective, and having a relatively high degree of accuracy when properly performed with suitable geometry samples), which is the major disadvantage of photoacoustic techniques. However, the problem inherent in the laser flash method is the involvement of comparatively large errors occasioned by the nonuniform radial distribution of the intensity of radiant heat emitted by the laser. Such serious errors can only be avoided by limiting to small sample sizes. Furthermore, to determine the values of some thin coatings or films, difficulties arise from extreme sensitivities associated with uncertainties and nonuniformity of the sample thickness, with possible gradations in properties of very thin films, and so on. Thus joining techniques are needed. Several alternate techniques, such as step heating, photoacoustic techniques, are good choices. For example, since the obvious advantage of photoacoustic techniques is the elimination of knowledge of coating thickness, photoacoustic techniques can be used to determine the values near room temperature and calculate the effective thickness of the layers for laser flash experiments [13,14]. In this paper, thermal diffusivity (δ) was measured on disk samples ($\varnothing 10 \times 2.0\ mm^3$) by laser flash method (Sinku-Riko Co. Model TC-7000) at room temperature. Furthermore, specific heat (C) was measured on disk samples ($\varnothing 6 \times 1.0\ mm^3$) by DSC (Perkin–Elmer Co, DSC-7 system) at room temperature. Also, bulk density (ρ) of specimen was measured by water displacement. For each measurement, three samples were tested three times. After that, thermal conductivity (λ) was calculated by equation:

$$\lambda = \delta \times C \times \rho$$

Morphological studies of SiC particles were carried out using transmission electron microscopy (TEM, JSM-2100) and field emission scanning electron microscopy (FE-SEM, LEO1550). SiC particles were coated with a thin gold layer before FE-SEM. Morphological studies of fracture surfaces of the nano-SiC/DGEBA/

EMI-2,4 composites were carried out also using FE-SEM (LEO1550). The nanocomposites were fractured in liquid nitrogen and then fracture surfaces were coated with a thin gold layer before FE-SEM.

3. Theoretical analysis

Enhanced characteristics in inorganic/polymer nanocomposites have been reported as a synergistic contribution from the effective combination of nanoparticles and matrix. Whether nanoparticles can bring positive effects into play depends on the joint contributions of particles dispersibility status in matrix and interfacial interaction [15]. An interlayer with covalent bonds would ensure an overall enhancement of properties, especially thermal conductivity, of the nanocomposites.

Interface structure can be tailored by selecting surface modification method of the particles. For all kinds of SiC particles, there is a native oxide layer of SiO_2 on the surface [16]. The content of SiO_2 and O^{2-} ions can be increased by oxidation. The O^{2-} ions exist as non-bridging oxygen: one bond connects with Si^{4+} and another bond forms a –OH group when reacting with H_2O, just as the following chemical equation [16]:

$$\equiv Si{-}O^- + H_2O \Leftrightarrow \equiv Si{-}OH + OH^-$$

Therefore, SiC particle is composed of five distinct layers. The first layer or inner core comprises SiC units. The second layer is the SiO_2 layer and is completely covered with silanol (SiOH) groups as the third layer. The fourth layer consists of water molecules, which are strongly bonded to the silanol groups. In the fifth layer, there is physically absorbed water, usually removed by drying or oxidation process. In general, after oxidation, the content of silanol (SiOH) groups on the SiC particles surface, OH^- groups absorbed on the SiC particles surface and the hydrogen bond absorbed water can be increased, and besides, the hydrophilic surface property of SiC particles is also enhanced.

In this paper, SiC particles were modified with A1100. The chemistry of silane treatment is described in many papers, and there are three models of grafting [17,18]. The most realistic (so-called "horizontal") one, as depicted in Fig. 3, involves the grafting reaction of silane and condensation: hydrolysis of the alkoxide groups of A1100 produces silanol (SiOH) groups and through condensation reactions, hydrolyzed molecules form siloxane bonds. These hydrolyzed molecules bond with SiC particles surface via hydrogen bonding to free surface silanol or siloxane [19], thus one end of A1100 forms hydrogen bonds with the SiC particles. As hydrogen bonds are heat-induced dehydrated, ≡Si–O–Si≡ bonds form between A1100 and SiC particles, and as a result, silane provides a network of covalent coupling among the SiC particles as well as several coupling agent molecular layers are grafted on the surface of SiC particles. Since aforesaid oxidation of SiC particles before silane treatment leads to more surface silanol (SiOH) groups, it is reasonable to expect more ≡Si–O–Si≡ bonds form between A1100 and SiC particles via the oxidation pretreatment. Furthermore, silane makes SiC agglomerates (in which aggregates are bound due to hydrogen and electrostatic bonding) decomposed, as the probability of strong hydrogen bonding and electrostatic interactions or condensation of ≡Si–OH groups markedly decreases. Thus grafted silanes reduce the agglomerate size of modified SiC and hydrophilic properties of SiC particles, improving particles' dispersibility status.

After surface modification, the treated SiC particles were blended with the epoxy resin. The other end of A1100, amidocyanogen, which is the polymerization-active group introduced onto particles, would enter in the epoxy macromolecule by means of chemical bond. Reactions between amine functionalized SiC (SiC–NH_2) particles and DGEBA, as depicted in Fig. 4, involve the

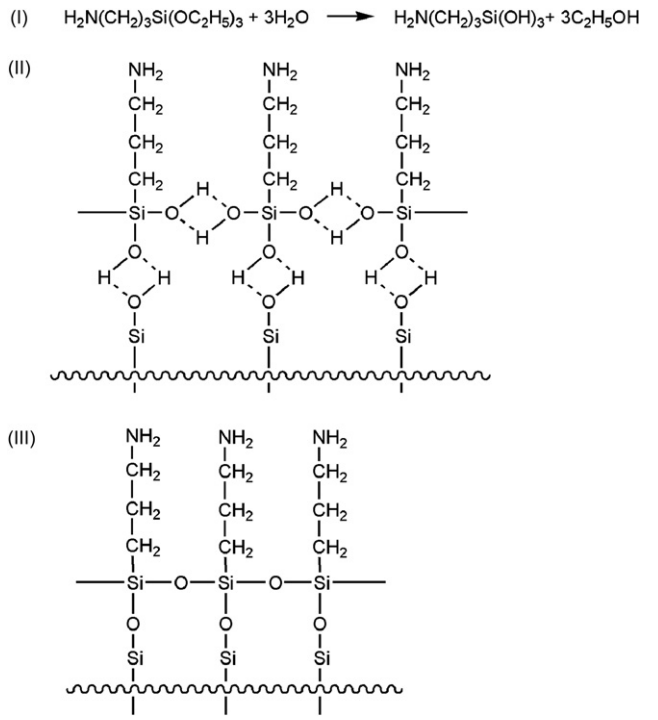

Fig. 3. Schematic presentation of (I) hydrolysis of A1100, (II) hydrogen bonding between SiC particle and A1100 and (III) oligomeric siloxane adsorption configuration for A1100 on SiC particle surface.

reactions between epoxide and amine hydrogen, forming OH-adducts, similar to the first step in the curing process of DGEBA/EMI-2,4 system, as depicted in Fig. 5 The resulting epoxy hydroxyl groups establish hydrogen bonds with silanol (SiOH) groups, and thereby forming ≡Si–O–C≡ bonds between SiC particles and epoxy matrix after dehydration. As a result, chemical bonding is build up at the SiC particles/resin interface. After the curing agent EMI-2,4 was added in the mixture, a cross-linked SiC particles/resin network, as depicted in Fig. 6, would form during the subsequent curing reaction. Fig. 6 was given just to show A1100 would form ≡Si–O–Si≡ and ≡Si–O–C≡bonds with SiC particles and epoxy matrix, respectively, as well as acting as curing agent and forming chemical bonds with epoxy. Despite other possible network configurations for the complexity of the reaction, it is definitely that cross-linked SiC particles/resin three-dimensional network would be formed by means of chemical bonds in the SiC/DGEBA/EMI-2,4 composites. The covalent bridge bonds would minimize the interfacial phonon scattering and contribute to heat conduction at interface, thus the network would be the efficient pathway for

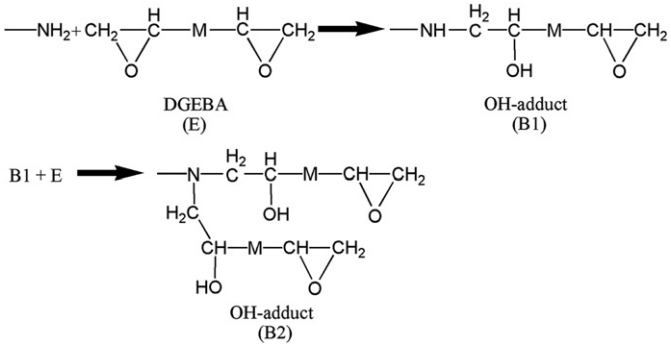

Fig. 4. Reactions between amine functionalized SiC (SiC–NH_2) particles and DGEBA.

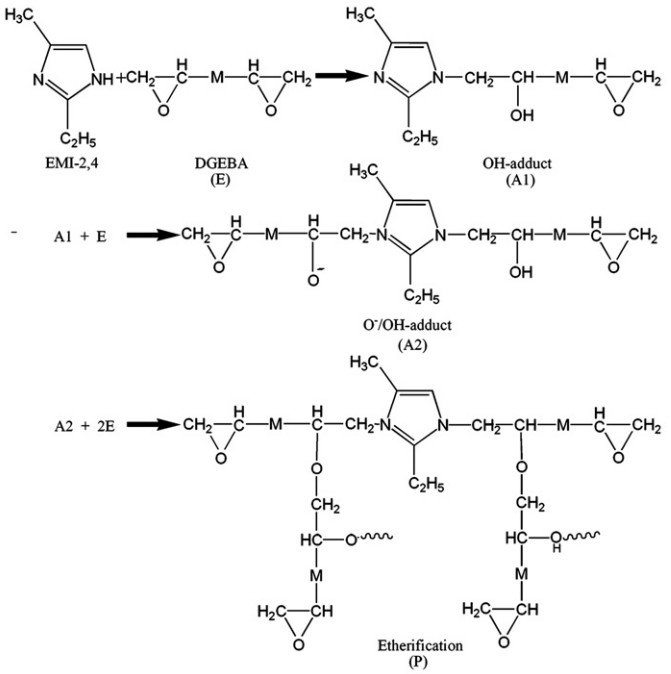

Fig. 5. Curing mechanisms for the DGEBA/EMI-2,4 system.

thermal diffusion, and play important role in improving thermal conductivity of the composites [6,7].

4. Results and discussion

Prior to study of the nanocomposites, surface feature of the treated nano-SiC particles should be known. Fig. 7 shows the FTIR spectra of untreated nano-SiC particles (Curve 1), silane treated nano-SiC particles (Curve 2), and oxidized plus silane treated nano-SiC particles (Curve 3). In this study, silane treated particles were washed with absolute ethanol repeatedly and then dried in vacuum, so in comparison with the spectrum of untreated particles (Curve 1), the emergence of additional characteristic absorptions of C–H stretching modes (multiple peaks at 2830–2960 cm^{-1}) [15] in Curves 2 and 3 confirms that the coupling agent has been covalently bonded to the nanoparticles as excepted. In addition, in Curves 2 and 3 there were no obviously new characteristic absorption of $–NH_2$ symmetric and asymmetric vibration at 2110

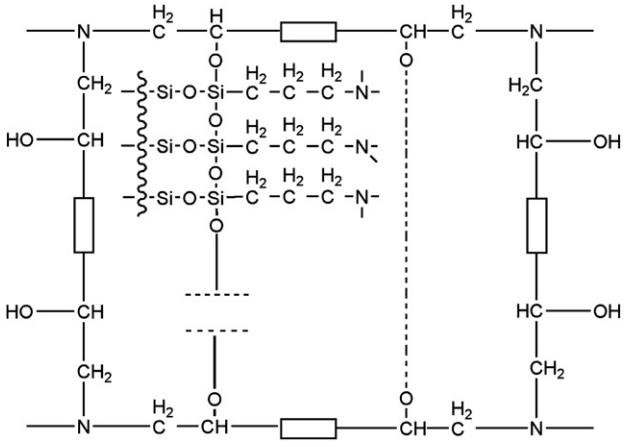

Fig. 6. Representative schematic network structure of the cross-linked silane (A1100) treated SiC/DGEBA/EMI-2,4 composites.

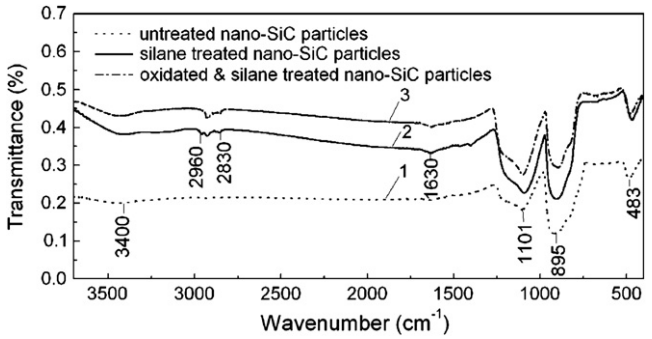

Fig. 7. FTIR spectra of nano-SiC particles. For the silane treated nano-SiC particles, the ungrafted silane coupling agent had been removed by solvent extraction before the FTIR measurement.

and 2357.5 cm^{-1}, respectively [19]. The reason may be due to the relatively small content of $–NH_2$ groups with respect to that of the Si–C bonds.

The peak at 895 cm^{-1} is the characteristic absorption peak of Si–C bonds of nano-SiC particles, while the peaks at 1101 and 483 cm^{-1} can be assigned to Si–O stretching vibrations and flexural vibrations, respectively [20–22]. In Curve 1, the existence of broad and strong absorption bands at 1101 and 483 cm^{-1} is an indication that the untreated nano-SiC particles have already had a relatively thick native SiO_2 oxide layer with respect to the size of nano-SiC particles. After surface treatment, there is a remarkable increase in relative intensity of 1101 cm^{-1} band with respect to that of the 895 cm^{-1} band. In Curve 2, the peak intensity at 1101 cm^{-1} approached that of Si–C bonds, which can be attributed to the formation of Si–O–Si bonds on the surface of nano-SiC particles after silane treatment, and in Curve 3, it increased slightly over that of Si–C bonds, which is due to the increased content of SiO_2 and Si–O–Si on the surface of nano-SiC particles after oxidation. The peak at 1101 cm^{-1} is composed of SiO_2 and Si–O–Si components [20–22].

In Curves 2 and 3, the stretching vibration band 3400 cm^{-1} of the hydroxyl group due to the noncondensed SiOH and/or unreacted –OH groups, and the flexural vibration band 1630 cm^{-1} of the hydrogen bond strengthened, illustrating that the hydroxyl group and the hydrogen bond absorbed on the nano-SiC particles surface were increased after surface treatment [16,23–25].

Fig. 8 shows the FTIR spectra of nano-SiC/DGEBA/EMI-2,4 composites. Several major differences are observed when compared with that of nanoparticles (Fig. 7). New infrared bands at 563, 829, 1508 and 1607 cm^{-1} are associated with characteristic adsorptions of phenyl [15]. New infrared bands at 1182 and 1246 cm^{-1} are related with epoxy and methylene twisting modes, respectively [25,26]. Characteristic absorptions of C–H stretching modes at 2830–2960 cm^{-1} moved to higher wave number

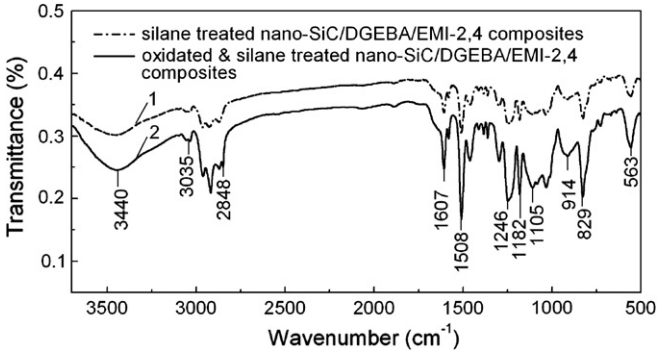

Fig. 8. FTIR spectra of nano-SiC/DGEBA/EMI-2,4 composites (14 vol.% filler content).

(multiple peaks at 2848–3035 cm^{-1}), and the stretching vibration band of the hydroxyl group shifted to 3440 cm^{-1}.

The peak of Si–O stretching moved from 1101 to 1105 cm^{-1}, verifying the formation of Si–O–C bonds between nano-SiC particles and epoxy resin. The adjacent peak at low wave number can be ascribed to the Si–O–Si bonds and SiO_2. No obvious existence of the peak ascribed to Si–C bonds can be due to two possible reasons. First, the peak shifted from 895 cm^{-1} to higher wave number and overlapped with the weak characteristic absorption peak of epoxy at 914 cm^{-1}. Second, the peak intensity of Si–C bonds decreased to the extent that it can't be comparable with that of Si–O stretching at 1105 cm^{-1}. Whencesoever, the dramatically decreased relative peak intensity of Si–C bonds with respect to that of the Si–O bonds strongly supports that there have been a great deal of covalent bonds of Si–O–C formed between nano-SiC particles and epoxy resin. Moreover, the strongly strengthened peak intensity of Si–O stretching at 1105 cm^{-1} in Curve 2 is the proof that the oxidation pretreatment of nano-SiC particles contributes to the formation of more Si–O–C structure in the nanocomposites.

Fig. 9 shows the FTIR spectra of micro-SiC particles (Curve 1) and micro-SiC/DGEBA/EMI-2,4 composites (Curve 2, containing the same filler content as the nanocomposites). In Curve 1, the prominent peak at 839 cm^{-1} and the slight shoulder peak at 943 cm^{-1} can be ascribed to Si–C vibrations [15], while the weak peaks at 1086 and 794 cm^{-1} can be assigned to Si–O vibrations [21], which include SiO_2 and Si–O–Si components. In this study, the oxidation time of micro-SiC particles is 10 times of that of nano-SiC particles, but in curve 1, compared with the infrared spectra of nano-SiC particles (Fig. 7), the relative peak intensity of Si–O bonds with respect to that of the Si–C bonds dramatically weakened, illustrating that the oxidation time of micro-SiC particles is still short, and compared with nano-SiC particles, the pretreatment of micro-SiC particles yields relatively thin SiO_2 oxide layer with respect to the size of micro-SiC particles, thereby yields a network of less covalent coupling (Si–O–Si bonds) among micro-SiC particles.

In Curve 2, the shift of Si–C stretching vibrations to lower wave number, 831 cm^{-1}, may be due to the influence of the characteristic absorption peak of epoxy groups at 830 cm^{-1}. The broad peak at 1070–1110 cm^{-1} indicates the formation of Si–O–C and Si–O–Si bonds, and it is much weaker than the peak of Si–C bonds, indicating that, compared with nano-SiC/DGEBA/EMI-2,4 composites, there are less Si–O–C and Si–O–Si bonds formed in the micro-SiC/DGEBA/EMI-2,4 composites.

The shift of Si–C stretching vibrations from 839 cm^{-1} (Fig. 9) to 895 cm^{-1} (Fig. 7) may be due to the size effect of quantum of nanomaterials, and the spectrum of nano-SiC particles shifts to higher wave number and results in "blue shift".

In summary, the FTIR results reported herein revealed that a cross-linked SiC particles/resin three-dimensional network was established by chemical bonding in the SiC/DGEBA/EMI-2,4 composites, and compared with micro-SiC/DGEBA/EMI-2,4 composites, there was a network of more covalent coupling, Si–O–Si and Si–O–C bonds, formed in the nano-SiC/DGEBA/EMI-2,4 composites. The reasons might be the high specific surface area (SSA) and highly active surface of nanoparticles.

The covalent bridge bonds minimize the interfacial phonon scattering and decrease the interface heat resistance by interpenetrating particles/resin interface. Therefore, the cross-linked SiC particles/resin three-dimensional network is an efficient pathway for thermal conduction. Besides, there is another thermal conduction pathway appearing at high filler content (greater than;the percolation threshold) as mentioned before, i.e., thermal conduction chains consisting of SiC particles. In this study, more covalent bonds were formed in the nano-SiC/DGEBA/EMI-2,4 composites, and this larger resulting network contributes to markedly higher thermal conductivity of nanocomposites than that of microcomposites at low filler content (nanocomposites with high filler content are difficult to manufacture for the poor dispersion of nanoparticles and poor castability caused by high viscosity), as shown in Fig. 10. Comparatively, treatment with silane only is more effective in improving thermal conductivity of the nanocomposites than oxidization and silane treatment. The reason may be the overgrown thick oxides, which dramatically decrease the whole native thermal conductivity of nano-SiC particles. Therefore, silane treatment only is the proper filler surface treatment approach for the nano-SiC/DGEBA/EMI-2,4 composites.

Based on the experimental results, it was concluded that it is the cross-linked SiC particles/resin three-dimensional network dominates the thermal conduction mechanism of nano-SiC/DGEBA/EMI-2,4 composites, which leads to nanocomposites with high thermal conductivity. Meanwhile, thermal conduction chains, the prevailing mean to conduct thermal diffusion in the micro-SiC/DGEBA/EMI-2,4 composites, are the secondary means to conduct thermal diffusion in the nanocomposites.

In this paper, the understanding of interface structure between SiC particles and resin enables us to understand the thermal conduction mechanisms, therefore guides us to choose proper filler surface treatment approaches to gain high thermal conductivity. Furthermore, it also guides us to design novel nanocomposites with higher thermal conductivity. Since the addition of nano-SiC particles to resin greatly enhances thermal conductivity at low filler contents, while micro-SiC particles significantly improve thermal conductivity of resin at higher filler contents (greater than percolation

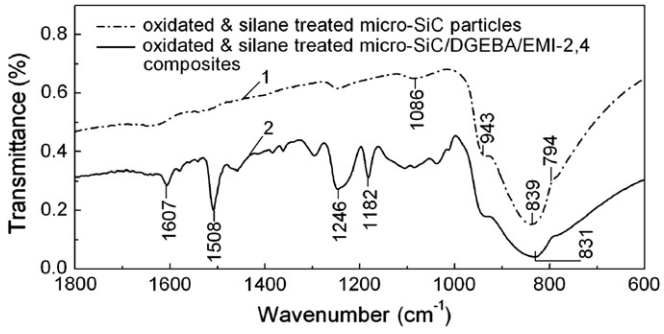

Fig. 9. FTIR spectra of micro-SiC particles and micro-SiC/DGEBA/EMI-2,4 composites (14 vol.% filler content).

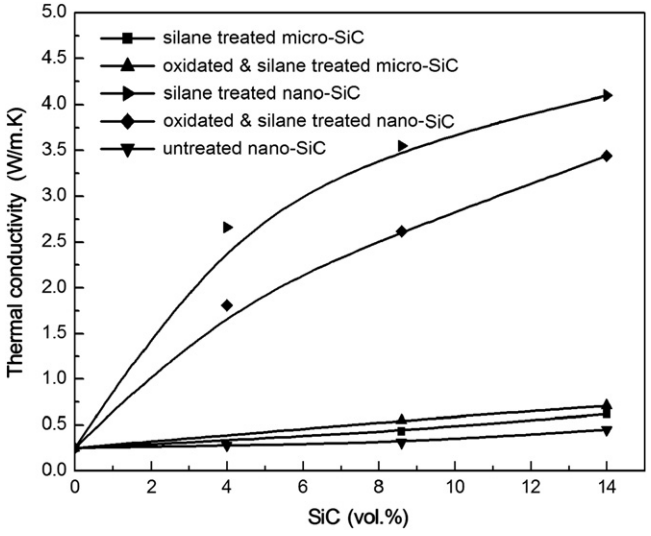

Fig. 10. Plot of thermal conductivity of SiC/DGEBA/EMI-2,4 composites vs. volume fraction of SiC particles. Lines are given only for showing the tendency.

threshold), it is reasonable to expect higher thermal conductivity of novel resin-based hybrid-filler composites (containing a mixture of nano-SiC and micro-SiC particles) resulting from the synergistic mechanism contributed from nano-SiC and micro-SiC particles.

5. Conclusions

Interfacial interaction plays a key role in composites performance. To intensify interfacial interaction, surface modifications of filler particles are utilized. However, general solutions do not exist. A specific strategy must be developed for each set of composites. In particular, recognition of proper surface modification would help to identify the mechanisms involved in the improvement of properties, such as thermal conductivity. In this paper, surface modification approaches included: (1) silane treatment using γ-aminopropyl-triethoxysilane (A1100) and (2) oxidation followed by silane treatment. The results showed that it is the cross-linked SiC particles/resin three-dimensional network dominates the thermal conduction mechanism of nano-SiC/DGEBA/EMI-2,4 composites, and leads to nanocomposites with high thermal conductivity. Meanwhile, thermal conduction chains, the prevailing mean to conduct thermal diffusion in the micro-SiC/DGEBA/EMI-2,4 composites, are the secondary means to conduct thermal diffusion in the nanocomposites. Silane treatment is the proper filler surface treatment approach for the nano-SiC/DGEBA/EMI-2,4 composites.

Acknowledgement

The authors are grateful for the financial support of National Natural Science Foundation of China (No.10776014), China Postdoctoral Science Foundation funded project (No.20080431103), High Technical Foundation of Jiangsu Province of China (No. BG2007047), Natural Science Foundation of Jiangsu Province of China (No. BK2008407), Jiangsu Planned Projects for Postdoctoral Research Funds (No.0801023B), Special Foundation for Young Scholars of Nanjing University of Science & Technology (No. AB41339) and Starting Foundation for Scholars of Nanjing University of Science & Technology (No. AB41980).

References

[1] Kirkpartick S. Reviews of Modern Physics 1973;45:574–88.
[2] Munson-McGee SH. Physical Review B 1991;43:3331–6.
[3] Celzard A, McRae E, Deleuze C, Dufort M, Furdin G, Mareché JF. Physical Review B 1996;53:6209–14.
[4] Gojny Florian H, Wichmann Malte HG, Fiedler Bodo, Kinloch Ian A, Bauhofer Wolfgang, Windle Alan H, et al. Polymer 2006;47(6):2036–45.
[5] Rong MZ, Zhang MQ, Ruan WH. Materials Science and Technology 2006;22(7):787–96.
[6] Clancy Thomas C, Gates Thomas S. Polymer 2006;47(16):5990–6.
[7] Hung Ming-Tsung, Choi Oyoung, Guo Zhanhu, Thomas Hahn H, Sungtaek Ju Y. Collection of technical papers–9th AIAA/ASME joint thermophysics and heat transfer conference proceedings, vol. 1; 2006. p. 719–25.
[8] Plueddemann EP. Silane coupling agents. New York: Plenum Press; 1991 [chapter 1].
[9] Neyman Elizabeth, Dillard John G, Dillard David A. The Journal of Adhesion 2006;82:331–53.
[10] Maxime J-F, Guinel M, Norton Grant. Journal of Materials Research 2006;21(10):2550–63.
[11] Eric Ramberg C, Cruciani Gary, Spear Karl E, Tressler Richard E, Ramberg Jr Charles F. Journal of the American Ceramic Society 1996;79(11): 2897–911.
[12] Zhou Tianle, Gu Mingyuan, Jin Yanping, Wang Junxiang. Polymer 2005;46:6216–25.
[13] Taylor RE. International Journal of Thermophysics 1998;19(3):931–9.
[14] Lin Bochuan, Li Chao, Su Chinghua, Ban Heng, Scripa Rosalia N, Lehoczky Sandor L. Proceedings of the ASME summer heat transfer conference, vol. 1; 2005. p. 777–85.
[15] Cai LF, Mai YL, Rong MZ, Ruan WH, Zhang MQ. Express Polymer Letters 2007;1(1):2–7.
[16] Shufan Ning, Hongyan Li, Wei Chen, Bin Liu, Shuoutian Chen. Rare Metals 2005;24(3):240–5.
[17] Ramier J, Chazeau L, Gauthier C, Guy L, Bouchereau MN. Journal of Polymer Science, Part B: Polymer Physics 2006;44:143–52.
[18] Sun Shuisheng, Li Chunzhong, Zhang Ling, Du HL, Burnell-Gray JS. European Polymer Journal 2006;42(7):1643–52.
[19] Sun J, Gao L. Dispersing. Journal of the European Ceramic Society 2001;21(13): 2447–51.
[20] Shi Liwei, Li Yuguo, Wang Qiang, Xue Chengshan, Zhang Huizhao. Rare Metal Materials and Engineering 2005;34(7):1073–6.
[21] Merle-Mejean T, Abdelmounim E, Quintard P. Journal of Molecular Structure 1995;349:105–8.
[22] Binsu VV, Nagarale RK, Shahi Vinod K. Journal of Materials Chemistry 2005; 15(45):4823–31.
[23] Sammon Chris, Bajwa Gurjit, Timmins Peter, Melia Colin D. Polymer 2006; 47(2):577–84.
[24] Mensitieri G, Lavorgna M, Musto P, Ragosta G. Polymer 2006;47(25):8326–36.
[25] Yu Jing, Wu Peiyi. Polymer 2007;48(12):3477–85.
[26] Shieh Yeong-Tarng, Liu Kuan-Han. Journal of Polymer Sciences, Part B: Polymer Physics 2004;42(13):2479–89.